ISSN 0965-545X, Polymer Science, Series A, 2025, Vol. 67:2. © Pleiades Publishing, Ltd., 2025.

MEDICAL POLYMERS

Synthesis, Characterization and Cytotoxicity Analyzes of Novel ABA–Type PNIPAM-*b*-PLLA-*b*-PNIPAM Amphiphilic Block Copolymer

Murat Mısır[a,]*, Serap Yalçın Azarkan[b], and Ahmet Bilgin[c]

[a] *Department of Chemical Engineering, Faculty of Engineering and Architecture, Kırşehir Ahi Evran University, Kırşehir, Türkiye*
[b] *Department of Medical Pharmacology, Faculty of Medicine, Kırşehir Ahi Evran University, Kırşehir, Türkiye*
[c] *Department of Mathematics and Science Education, Faculty of Education, Kocaeli University, Kocaeli, Türkiye*
**e-mail: murat.misir@ahievran.edu.tr*

Received July 22, 2024; revised May 11, 2025; accepted May 22, 2025

Abstract—ABA–type amphiphilic poly(*N*-isopropylacrylamide)-*block*-poly(L-lactide)-*block*-poly(*N*-isopropylacrylamide) (PNIPAM-*b*-PLLA-*b*-PNIPAM) was synthesized via combination of ring opening polymerization (ROP) and atom transfer radical polymerization (ATRP) using the novel bifunctional PLLA–based ATRP macroinitiator bearing 1,2-bis[(3-oxapropyl)oxa]benzene core. For this purpose, at first bifunctional diol initiator, *o*-bis[(3-hydroxypropyl)oxy]benzene **(1)**, was synthesized by the reaction of catechol and 3-chloro-1-propanol in the presence of sodium hydroxide (NaOH) in ethanol. Secondly, PLLA-diol (HO-PLLA-OH) was prepared by $Sn(Oct)_2$ -catalyzed (ROP) of (L-LA) at 120°C using (1) as initiator in toluene. Thirdly, dibromoester end-functionalized PLLA-based ATRP macroinitiator (Br-PLLA-Br) was synthesized by esterification of hydroxyl end groups of PLLA-diol. Finally ABA-type block copolymer, (PNIPAM-*b*-PLLA-*b*-PNIPAM), was synthesized by (ATRP) of NIPAM as monomer using PLLA-based ATRP macroinitiator in presence of copper(I) chloride/tris[2-(dimethylamino)ethyl]amine ($CuCl/Me_6TREN$) as catalyst system in DMF/water at 25°C. Characterization of the molecular structures for synthesized novel macroinitiator and the block copolymer were made by spectroscopic (FTIR and ^1H NMR) and chromatographic (GPC) methods. In the application phase of this study, the effectiveness of polymers was examined on cancer cells. Cytotoxicity and metastatic effects were evaluated in vitro on MDA-MB-231 cell lines. As a result, novel ABA-Type PNIPAM-*b*-PLLA-*b*-PNIPAM amphiphilic block copolymer, which has been successfully developed, characterized and determined to be non-toxic, can be used as a promising drug delivery system in many areas such as tumor treatments.

DOI: 10.1134/S0965545X24600698

INTRODUCTION

Chemotherapy continues to be the predominant approach in cancer treatment, employing anticancer agents to impede the proliferation of malignant cells [1, 2]. Nevertheless, the current roster of authorized medications [3, 4] remains constrained, primarily due to common severe side effects, limited bioavailability, poor water solubility, and inadequate targeting efficacy. To overcome this challenge, scientists have developed different strategies for delivering chemotherapy drugs, including nanoparticle-based systems. Nanomedicine is emerging as a pivotal approach for drug delivery and disease imaging, aiming to enhance therapeutic effectiveness while minimizing side effects [5–7]. Within this field, polymeric nanocarriers have garnered significant attention due to the wide array of polymeric materials available, their amenability to functionalization with targeting or imaging groups, the ease of adjusting physicochemical properties for nanocarrier design, and the potential for incorporating stimuli-responsive features to enable controlled drug release [8, 9].

Presently, there is a thorough exploration into the advancement of polymer nanoparticles for drug conveyance and detection systems [10–12]. The key benefits of polymer systems over inorganic materials include their structural and property diversity, heightened drug-loading capabilities, and the array of reactive functional groups for biomolecule-vector attachment. Furthermore, most polymer systems exhibit predictable degradation mechanisms, in contrast to many inorganic materials that tend to accumulate in the body. Among the broad spectrum of biocompatible and biodegradable polymers employed in nanoparticle formulation, amphiphilic copolymers facilitate the straightforward creation of nanostructures with various morphologies (polymersomes, micelles, and nanospheres) owing to their self-assem-

bling ability in aqueous environments [13–15]. Self-assembled nanoparticles are adept at encapsulating hydrophobic, hydrophilic, and amphiphilic drugs [16–18]. Presently, a diverse range of amphiphilic copolymers with varying structures and compositions have been delineated and deliberated [13, 19, 20]. Although there are many known amphiphilic copolymers, only a limited subset can be considered suitable candidates for drug delivery. For safety, nanoparticles proposed for in vivo use must be biocompatible, preferably biodegradable, with predictable mechanisms for elimination from the body [21].

Among controlled/living radical polymerization (CRP) techniques, ATRP has found a great usage for macromolecular design using halogen containing initiators [22–24] ATRP method has been demonstrated for the controlled polymerization of different monomers which include a variety of functional groups, such as styrene [25, 26], acrylate [27, 28] and methacrylate [29]. Also, this method provides the control for variations in composition and architecture [30].

The combination of ROP and ATRP has received remarkable attention with regard to macroinitiator and block copolymer synthesis [31]. ROP can be performed both in a controlled and living manner, depending on the monomer and initiator/catalyst system [30]. Aliphatic polyesters such as poly (lactic acid) (PLA) and poly(ε-caprolactone) (PCL) are interesting polymers for pharmacological, biomedical, environmental, and agricultural applications due to their good mechanical properties, hydrolyzability and biocompatibility [32, 33]. Recently, copolymers and blends of PLA (poly lactide) have been studied to enhance their mechanical, thermal or biodegradability properties. During the last years, copolymers based on polyester and PNIPAM with advanced macromolecular architectures have also been investigated as carriers for drug delivery system, copolymerization of PNIPAM with lactide allows the combining the thermosensitivity of PNIPAM and degradability of PLA [34].

Polylactides are well-known hydrophobic, biodegradable, and biocompatible aliphatic esters, which are nontoxic for the human body. Polylactides have been used in biomedical and pharmaceutical applications as bioresorbable sutures, scaffolds in tissue engineering matrices for controlled drug delivery systems [34, 35]. Poly(*N*-isopropylacrylamide) (PNIPAM) is a thermosensitive polymer with a lower critical solution temperature (LCST) of ~32°C. It is extensively employed to form the temperature-responsive copolymers with other polymers [36]. The advancements in synthetic methods have made the synthesis of various kinds of di- and tri-block copolymers. Until recently, most of the studies have focused on preparation of AB-type [36, 37] diblock or ABA-type [34] or ABC-type [38] triblock copolymers containing PLA and PNIPAM using many polymerization routes, have been studied extensively by many researchers.

We report synthetic approach to BCPs via combination of ROP and ATRP using a novel bifunctional initiator for preparation of ABA-type PNIPAM-*b*-PLLA-*b*-PNIPAM BCPs. Firstly, HO–PLLA–OH (Poly L-lactide) diol synthesized by $Sn(Oct)_2$ -catalyzed ROP of L-LA in toluene using a novel bifunctional initiator not used in initiation step of any polymerization. Secondly, dibromoester end-functionalized PLLA macronitiator was prepared by esterification of hydroxyl end groups of PLLA diol. ABA-type PNIPAM-*b*-PCL-*b*-PNIPAM BCP was synthesized by ATRP of NIPAM as monomer using PLLA-based macroinitiator and $CuCl/Me_6TREN$ as catalyst system in DMF/water at 25°C.

In this study, to evaluate the potential of developed drug delivery systems, we established the characteristics and morphology of these, which depend on the polymer composition. Additionally, we assessed their cytotoxicity and metastatic properties on MDA-MB-231 (human breast adenocarcinoma, triple-negative breast cell) cancer cells.

EXPERIMENTAL

Materials

Reactions were performed under an atmosphere of argon using standard Schlenk techniques unless otherwise specified. *N*-isopropylacrylamide (NIPAM) (Sigma-Aldrich, 97%), was purified by re-crystallization from *n*-hexane/toluene mixture and dried in vacuum. L-lactide (L-LA) (TCI, 98%) was purified by recrystallization from ethyl acetate/*n*-hexane twice and dried in vacuum at room temperature and kept in freezer. Copper(I) chloride (CuCl) (98%; Aldrich) was purified by stirring overnight in glacial acetic acid to remove Cu^{2+}, after filtered and washed with ethanol, and then dried in vacuo at 70°C for two days. Tris[2-(dimethylamino)ethyl]amine (Me_6TREN) was synthesized according to published procedure [39]. 2-Bromopropionyl bromide (Sigma-Aldrich, 97%), triethylamine (TEA, 99.5%, Aldrich), 3-chloro-1-propanol (TCI, 98%), catechol (99%, TCI), dichloromethane (DCM), stannous octaonate $Sn(Oct)_2$ were used as received. 2,2'-Azobis(isobutyronitrile) (AIBN) was received from TCI > 98%. After recrystallization from methanol it was stored at 4°C. Conventional procedures were used for purification of all solvents [40].

Measurement

FTIR spectra were recorded using a Thermofisher Scientific Nicolet IS50 spectrometer. ^1H NMR spectra were recorded on a Varian XL-400 NMR spectrometer and chemical shifts were reported (δ_H) relative to tetramethylsilane as the internal standard. The number-average molecular weight M_n(GPC) and molecular weight distribution ($Đ$) values were ana-

lyzed by GPC, using Shimadzu LC-2050C LT GPC system with column (Shimadzu Shim-pack GPC 804, THF LC Column 300 × 8.0 mm) in THF calibrated with PMMA standards at 25°C. THF (HPLC grade) was used as an eluent at a flow rate of 1.0 mL/min for GPC analyses.

Synthesis of o-Bis[(3-hydroxypropyl)oxy]benzene (1)

o-Bis[(3-hydroxypropyl)oxy]benzene (1) was synthesized by the reaction of catechol and 3-chloro-1-propanol in, according to previously published procedure [41]. (Yield: 79%, yellow-brownish solid, m.p. 51–53°C; FTIR (KBr), cm^{-1}: 3400 (−OH), 3342 (H−O···H), 3080 (=CH aromatic), 2959-2814 ($-CH_2$ aliphatic), 1593 (aromatic −C=C−), 1510, 1479, 1465, 1454, 1398, 1331, 1257 (Ar−O−CH_2), 1220, 1124, 1056 (Primary alcohol, C−O), 989, 956, 746; ^{1}H NMR ($CDCl_3$), δ_H, ppm: 6.86–6.82 (m, 4H, Ar**H**), 4.11 (t, 4H, C$\mathbf{H_2}$−O−Ar), 3.80 (t, 4H, O−CH_2−CH_2−C$\mathbf{H_2}$−OH), 1.99 (p, 4H, O−CH_2−C$\mathbf{H_2}$−CH_2−OH), 1.68 (s, br, 2H, O−CH_2−CH_2−CH_2−O**H**).

Synthesis of PLLA-OH in the Presence of Novel Initiator (1) via ROP

The reaction mechanism is shown in Scheme 1. HO-PLLA-OH was synthesized via ROP of L-LA as follows: into the ROP initiator (1) (0.226 g, 1 mmol), L-lactide (2.94 g, 20 mmol) and $Sn(Oct)_2$ (3.41×10^{-3} mL, 0.01 mmol) in dry toluene (5 mL) were introduced into the 25 mL Schlenk flask equipped with a magnetic stirrer. The reaction mixture was further degassed by three freeze-pump-thaw cycles. The flask was then placed into preheated constant-temperature oil bath at 120°C for 24 h. The crude polymer was dissolved in a small amount of DCM and then precipitated into excess of cold hexane. The resulting white powder polymer was collected by filtration and drying in the vacuum oven at room temperature until constant weight.

Yield: 2.91 g, Conversion: 91%. M_n(theo.): 2857 g/mol; M_n(NMR): 3100 g/mol; M_n(GPC): 4500 g/mol; *Đ*: 1.44; FTIR (ATR) cm^{-1}: 3515, 2995, 2945, 1755, 1455, 1359, 1183, 1130, 1087, 1043, 872, 755, 695; ^{1}H NMR ($CDCl_3$) δ_H, ppm: 6.89 (Ar**H**), 5.16 (−C**H**(CH_3)OCO) H^d)], 4.37–4.32 [(−C**H**(CH_3)OH, $H^{d'}$) + (C$\mathbf{H_2}$−O−Ar, (H^a)], 4.04 (−O−CH_2−CH_2−C$\mathbf{H_2}$−O, H^c), 2.13 (−O−CH_2−C$\mathbf{H_2}$−CH_2−O, H^b), 1.57 (−CH(C$\mathbf{H_3}$)OCO−, H^e), 1.49 (−CH(C$\mathbf{H_3}$)OH, $H^{e'}$.

Synthesis of Br-PLLA-Br

PLLA-Br macroinitiator was synthesized by esterification of PLLA diol using 2-bromopropionyl bromide in the presence of TEA. Typically, a 100 mL two-necked round-bottom flask was charged with PLLA-OH (1.162 g, 0.375 mmol, M_n(NMR) = 3100 g/mol) was dissolved in dry DCM (20 mL) with TEA (0.263 mL, 1.875 mmol) while stirring under argon atmosphere. 2-Bromopropionyl bromide (0.121 mL, 1.125 mmol) was added dropwise to the cooled reaction mixture at 0°C for 30 min. The reaction mixture was stirred at room temperature for 72 h. The precipitated salt was removed by filtration, then the filtrate was diluted with 20 mL DCM. The mixture was washed with 5% aqueous $NaHCO_3$ (3 × 20 mL) and then water (3 × 30 mL) and finally dried over $MgSO_4$. The concentrated solution was precipitated into excess of cold methanol and the product was dried in vacuum. M_n(NMR) = 3745 g/mol. M_n(GPC) = 5440 g/mol; *Đ*: 1.44. Yield 1.14 g, 81%.

Synthesis of PNIPAM-b-PLLA-b-PNIPAM via ATRP

PNIPAM-*b*-PLLA-*b*-PNIPAM TBC was prepared using PLLA-Br macroinitiator by ATRP. Typically, 0.122 g (0.0325 mmol, M_n(NMR) = 3745 g/mol) of PLLA-Br, NIPAM 569 mg (4.875 mmol) and 6.5 mg (0.065 mmol) CuCl were dissolved in 1.5 mL DMF, then 0.3 mL H_2O were introduced into a 25 mL Schlenk tube. After three freeze-pump-thaw cycles, 17.1 μL (0.065 mmol) Me_6TREN were added under argon atmosphere. The reaction was then allowed to proceed under stirring at 25°C for 0.5 h. After quenching with liquid nitrogen, viscous solution was precipitated by adding of diethyl ether. The crude product was dissolved in DCM. The catalyst was removed by passing the dilute solution through a neutral alumina column. The resulting colorless solution was then concentrated, followed by precipitation in cold diethyl ether. The final product was dried under vacuum at room temperature for 48 h.

Yield: 0.35 g, Conversion: 40%. M_n(theo.): 9900 g/mol; M_n(NMR): 8770 g/mol; FTIR (ATR), cm^{-1}: 3293, 3070, 2972, 2924, 1756, 1638, 1536, 1455, 1365, 1183, 1088, 1043, 872, 837; ^{1}H NMR ($CDCl_3$) δ_H, ppm: 6.57 (−N**H**CH(CH_3)$_2$, H^j), 5.13 (−C**H**(CH_3)OCO) H^d)], 3.97 (−C**H**(CH_3)$_2$, H^k), 2.12 (−CH_2−C**H**−, H^i), 1.79 (−C$\mathbf{H_2}$−CH−, H^h), 1.56 (−CH(C$\mathbf{H_3}$)OCO−, H^e), 1.12 (−CH(C$\mathbf{H_3}$)$_2$, H^l).

Cell Culture

For this study, breast cancer (MDA-MB-231) and MCF10A healthy breast epithelial cell lines were utilized. These cell lines were sourced from the Medical Pharmacology Department of Kırşehir Ahi Evran University. The cells were cultured at 37°C with 5% CO_2 in RPMI medium supplemented with 10% Fetal Bovine Serum and 1% penicillin-streptomycin.

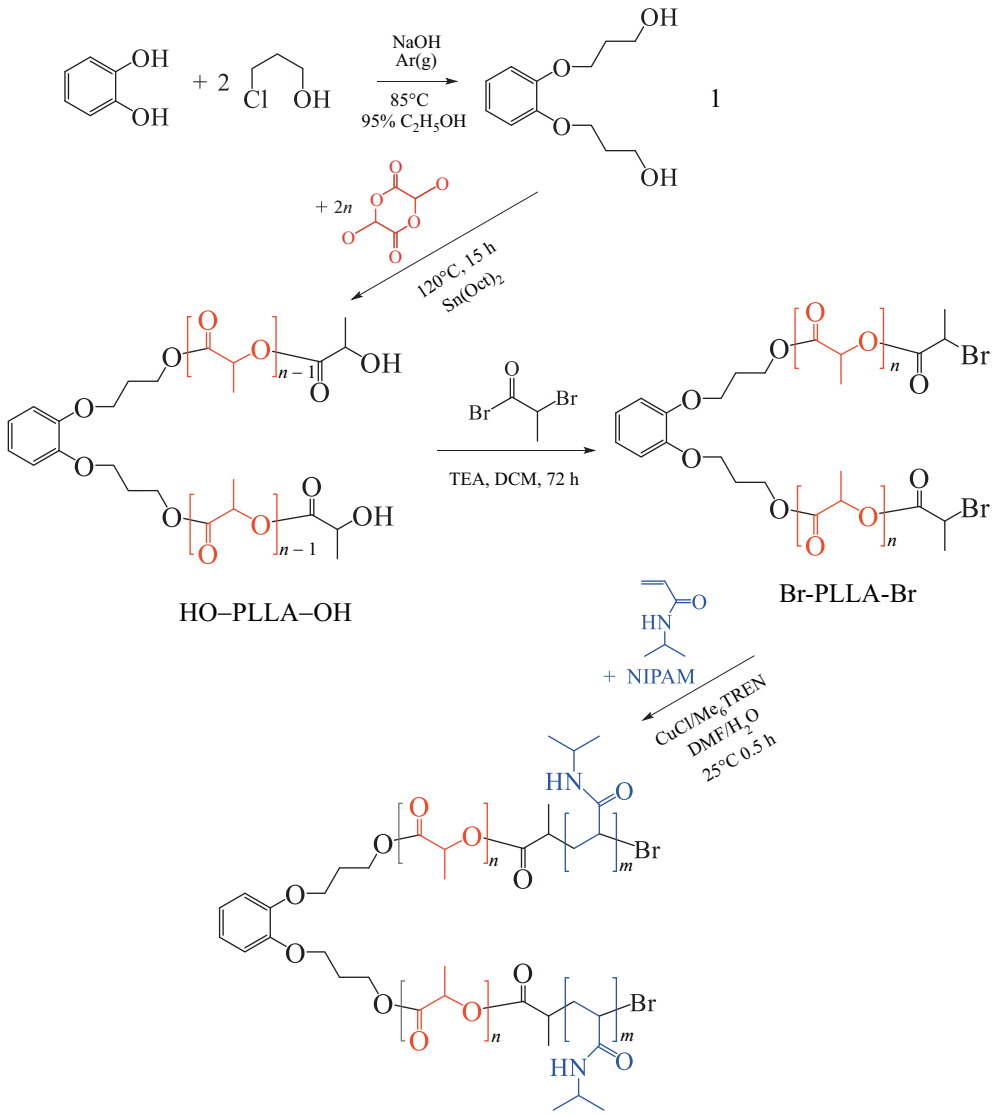

Scheme 1.

Cytotoxicity Analyses

The cytotoxic impact of copolymer MDA-MB-231 cells was assessed using the XTT assay kit (Biological Industries, USA). 8000 cells were seeded per well in a 96-well plate. Following a 24-hour incubation period, the cells were exposed to copolymer. After 72 h of incubation, the solutions from the XTT kit were introduced to the cells. Cell viability was then measured using a microplate reader (BIOTEK ELX808, USA) at a wavelength of 450 nm. The IC50 value was determined. The inhibition rates of cells, as a result of the readings, were calculated using the following formula: % inhibition: (A450 nm test – A450 nm control/A450 nm control) ×100.

Wound Healing Assay

1.5×10^5 cells were seeded in 6-well plates and incubated at 37°C with 5% CO_2 for 48 h. When the cells reached 80% confluence, wounds were created using a 20–200 μL pipette tip [18]. Subsequently, 4 mL of fresh medium and 1 mL of copolymer were added. The closure of the wounds was monitored and captured using an inverted microscope (BAB, Türkiye).

Invasion Assay

Cell culture inserts were positioned in 24-well plates, and 100 μL of a pre-prepared stock of 1 : 10 matrigel was applied. The plate was then incubated for 48 h at 37°C to achieve a gel-like consistency. Once the desired structure was formed in the matrigel,

RPMI-1640 medium containing fetal bovine serum (FBS) was added to the wells. Serum-free RPMI-1640 medium was added to the matrigel-containing insert, and approximately 10^6 cells were inoculated. Copolymer were placed in wells containing medium with serum and incubated at 37°C for 48 h. After incubation, the cells were treated with 10% formaldehyde for 10 min, followed by staining with Giemsa [42].

RESULTS AND DISCUSSION

PNIPAM-*b*-PLLA-*b*-PNIPAM triblock copolymer was synthesized via combination of ROP and ATRP in three steps: (i) ROP of L-LA, (ii) esterification of PLLA diol, and (iii) polymerization of NIPAM via ATRP. Firstly, dihydroxyl-terminated PLLA ([monomer]/[initiator] = 20) was synthesized ROP of L-LA, as the monomer, initiated by (1) in the presence of $Sn(Oct)_2$ at 120°C for 15 h. HO-PLLA-OH was characterized by FTIR and ^{1}H NMR.

FTIR spectra of PLLA and block copolymer are shown in Fig. 1. As seen Fig. 1 (curve *1*), the characteristic absorption peak of the carbonyl group at around 1755 cm^{-1} with high relative intensity, arising the formation of the ester carbonyl bond, is PLLA block units, indicating the polymerization of L-LA. The spectrum also showed two bands at 2995–2935 cm^{-1}, representing symmetric and asymmetric C–H stretching of $-CH_3$, respectively. The bands at 1454 and 1359 cm^{-1} represent the stretching of C–H in methyl group of PLLA. The peaks at 1183 and 1087 cm^{-1} are attributed to (C–O) and (–C–O–C) stretching. The bands observed at 872 and 755 cm^{-1} can be attributed to amorphous and crystalline phases of PLLA [43].

^{1}H NMR spectrum of bifunctional PLLA is shown in Fig. 2a. In the ^{1}H NMR spectrum of HO–PLLA–OH the peaks of methine (H^d) and methyl (H^e) protons, corresponding to PLLA repeating unit, were detected at 5.16 and 1.57 ppm, respectively.

It can be seen that the peak of methylene protons neighboring to oxygen atoms ($C\mathbf{H_2}$–O–Ar, (H^a)) shift from δ_H = 4.11 to δ_H = 4.37–4.32 ppm and overlap with that of terminal methine ones ($H^{d'}$) in PLLA block. The signals assigned to methylene protons of initiator fragment shifted to δ = 4.04 (–O–CH_2–CH_2–$C\mathbf{H_2}$–O, H^c) and 2.13 (–O–CH_2–$C\mathbf{H_2}$–CH_2–O, H^b) ppm are observed as a result of polymerization in PLLA. The peak at 6.89 ppm (Ar–H, H^{ArH}) is attributed to the aromatic methylene protons in initiator 1 fragment.

For PLLA–OH, the number-average molecular weight M_n(NMR) calculated by comparing the peak integrals derived from the methyl proton peaks of PLLA (δ_H = 5.16 ppm) and the methylene proton peaks of initiator (peak c in Fig. 2a) is close to the theoretical number-average molecular weight M_n(theor.).

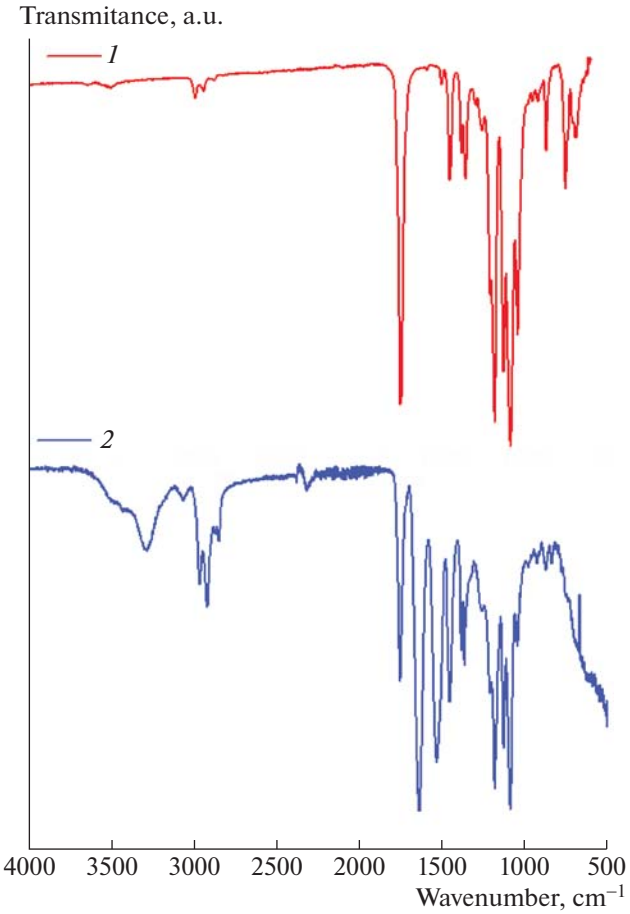

Fig. 1. The FTIR spectra of (*1*) HO–PLLA–OH and (*2*) PNIPAM-*b*-PLLA-*b*-PNIPAM.

M_n(NMR) of PLLA was calculated by integral area of related peaks displacements according to Eq. (1):

$$M_n(\text{NMR}) = \frac{I_c}{I_d} M_{\text{monomer}} + M_{\text{initiator}}, \quad (1)$$

where, M_{monomer} and $M_{\text{initiator}}$ are molecular weights of the L-lactide and initiator, respectively.

The theoretical number-average molecular weight M_n (theor.) was calculated by according to Eq. (2):

$$M_n(\text{theor.}) = \frac{[M]}{[I]} M_{\text{monomer}} \times \text{Conversion}(\%) + M_{\text{initiator}}. \quad (2)$$

In the second step, dibromoester functionalized PLLA macroinitiator was prepared by esterification of hydroxyl end groups of PLLA with 2-bromopropionyl bromide in the presence of TEA. In the ^{1}H NMR spectrum of PLLA-Br (in Fig. 2b), the new two signals appeared at 4.43 (H^f) and 1.85 (H^g) ppm, corresponding to methine protons and methyl protons of bromo propionate end, respectively. The disappearance of peak at 4.36 ppm, corresponding to the methine pro-

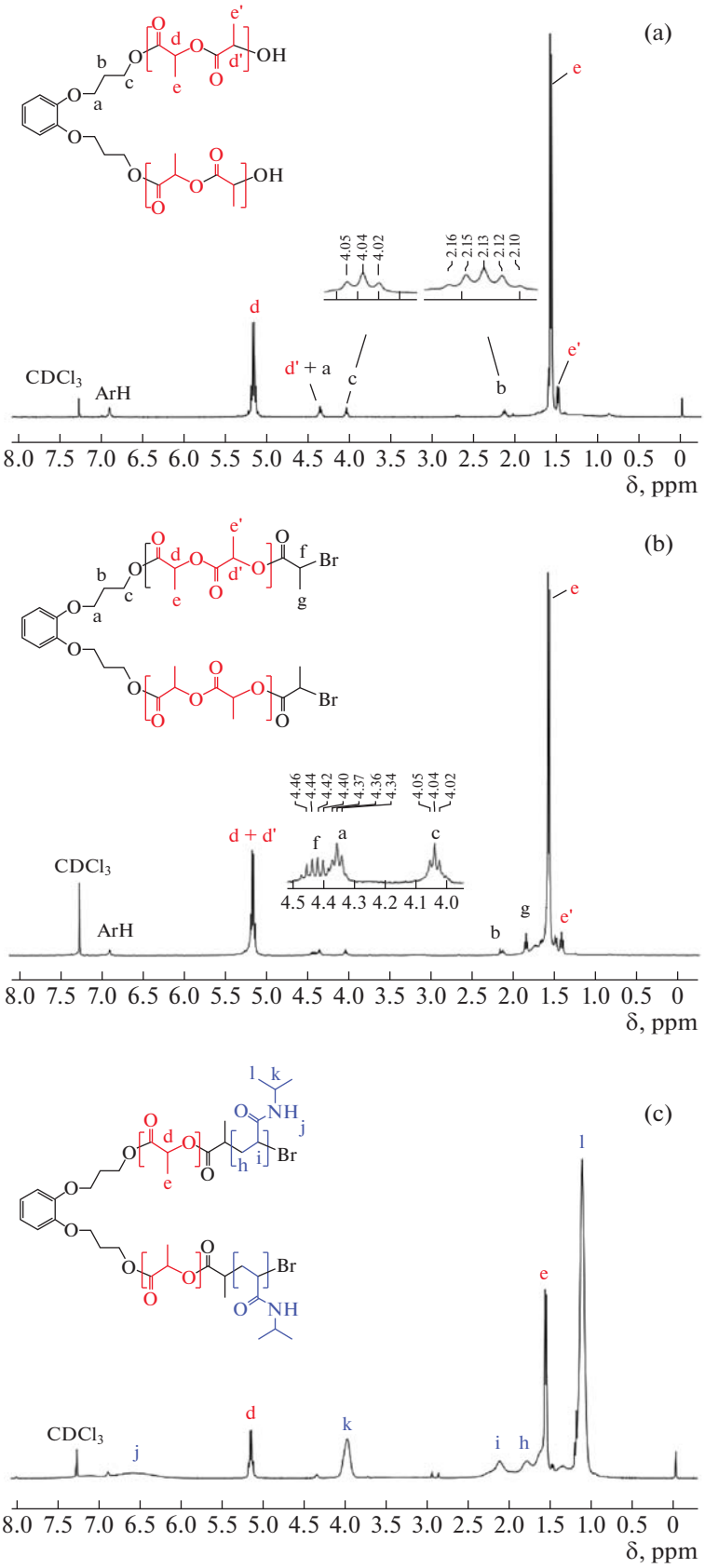

Fig. 2. The NMR spectra of (a) HO–PLLA–OH, (b) Br-PLLA-Br, and (c) PNIPAM-*b*-PLLA-*b*-PNIPAM.

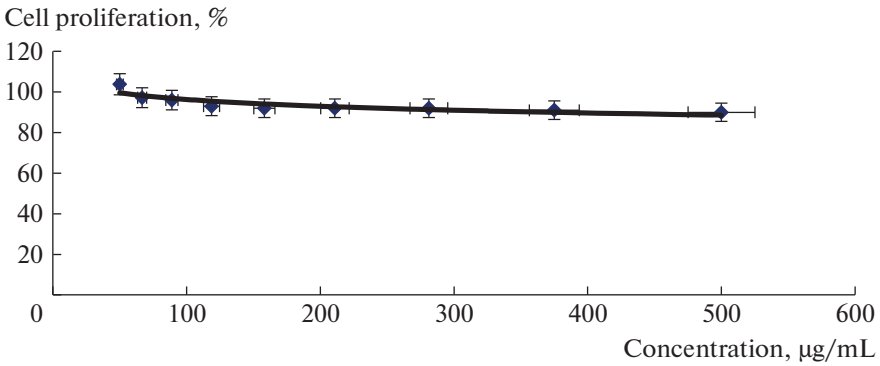

Fig. 3. Cytotoxicity analysis of PNIPAM-*b*-PLLA-*b*-PNIPAM.

tons adjacent to terminal hydroxyl end groups of PLLA end, indicates that the esterification was successful. The resonance peaks of repeating methine and methyl protons of the PLLA main chain at 5.16 (H^d) and 1.58 (H^e) ppm were detected with high resolution, respectively. The triplets appearing at δ_H = 4.36 and 4.04 ppm in the spectrum were assigned to methylene protons (−O−C**H**$_2$−CH$_2$−CH$_2$−OH, H^a) and (O−CH$_2$−CH$_2$−C**H**$_2$−O, H^c), respectively. The spectrum also gave signals at δ =2.14 ppm for methylene (−O−CH$_2$−C**H$_2$**−CH$_2$−O, H^b) and at δ = 6.90 ppm for the aromatic (Ar−**H**, H^{ArH}) protons of initiator 1.

The number-average molecular weight M_n (NMR) of PLLA-Br calculated by comparing the peak integrals derived from the methine proton peaks of PLLA (δ = 5.18 ppm) and the methylene proton peaks of initiator (peak c in Fig. 2b) according to Eq. (3):

$$M_n(\mathrm{NMR}) = \frac{I_e}{I_c} M_{\mathrm{monomer}} + M_{\mathrm{initiator}} + M_{\mathrm{bromine\text{-}end\ group}}, \quad (3)$$

where M_{monomer}, $M_{\mathrm{initiator}}$ and $M_{\mathrm{bromine\text{-}end\ group}}$ are molecular weights of the L-lactide, initiator and bromine-end group, respectively.

In the third step, PNIPAM-*b*-PLLA-*b*-PNIPAM triblock copolymer was synthesized by ATRP of NIPAM as monomer using PLLA-Br as macroinitiator and CuCl/Me$_6$TREN as catalyst system in DMF/water at 25°C with molar ratio of monomer to initiator, i.e. [M]/[I] =150. FTIR spectrum of block copolymer is shown in Fig. 1 (curve *2*). In the spectrum of block copolymer, appearance of the characteristic absorption peak of the carbonyl group at around 1756 cm^{-1}, corresponding to PLLA units, indicated that block copolymer was formed. The observation of the peaks at 3293 cm^{-1} (N−H stretching), 1638 cm^{-1} (C=O stretching) and 1536 cm^{-1} (N−H bending) belonging to PNIPAM unit support the formation of block copolymer [44].

^{1}H NMR spectrum of PNIPAM-*b*-PLLA-*b*-PNIPAM displayed characteristic signals at 3.97 and 1.12 ppm assigned to the methine (H^k) and methyl (H^l) protons of PNIPAM, respectively. The signals at 5.13 and 1.56 ppm were ascribed to methine and methyl protons of PLLA, respectively. A broad signal peak appeared at 6.57 ppm (H^j), which show the presence of proton of −NH group. The signals at δ_H = 2.12 (H^i) and 1.79 (H^h) ppm are also attributed to the methine and methylene group of PNIPAM unit, respectively.

M_n(NMR) of PNIPAM-*b*-PLLA-*b*-PNIPAM was calculated by comparing the peak integrals derived from the methine proton peaks of PNIPAM (δ_H = 3.97 ppm, peak k) and the methyl proton peaks of PLLA (δ_H = 5.13 ppm, peak d in Fig. 2c) according to Eqs. (4) and (5):

$$M_n(\mathrm{NMR}) = DP_{\mathrm{PNIPAM}} M_{\mathrm{monomer}} + M_{\mathrm{n,PLLA}}, \quad (4)$$

$$DP_{\mathrm{PNIPAM}} = \frac{I_k}{I_d} DP_{\mathrm{PLLA}}, \quad (5)$$

where DP_{PNIPAM} and DP_{PLLA} are degree of polymerization for PNIPAM and PLLA segments, respectively. M_{monomer} is also molecular weight of the NIPAM.

In vitro Analyses

In vitro cytotoxicity evaluation in cancer cells is a crucial assay to evaluate the potential activity and toxicity of new drug carriers [45]. XTT analysis was performed to determine the cytotoxic effect of amphiphilic block copolymer on breast cancer cells. As a result of the cytotoxicity analysis, no toxic effect of amphiphilic block copolymer was observed on the breast cancer cell line. The results obtained are shown in Fig. 3.

The inhibitory effects of the amphiphilic block copolymer on the migration and invasion of tumor cells were initially evaluated using wound healing and invasion assays. The wound healing assay is a simple and inexpensive method that experimentally mimics cell growth and migration, leading to wound closure.

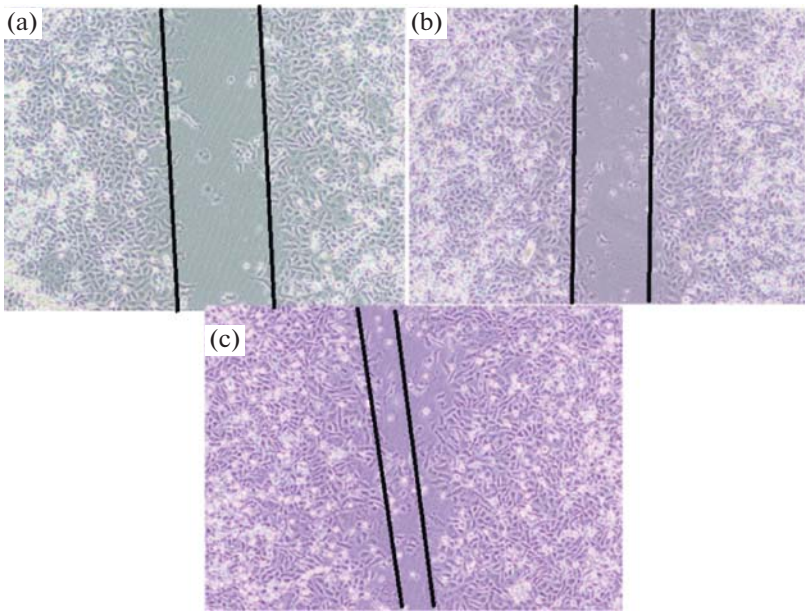

Fig. 4. Control group: (a) 24, (b) 48, (c) 72 h.

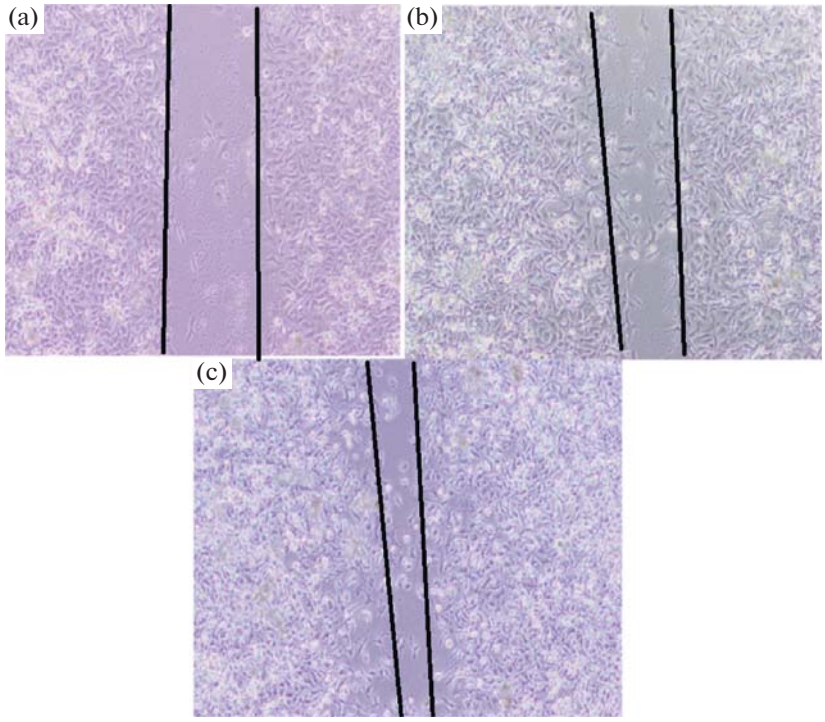

Fig. 5. Copolymer treated cells: (a) 24, (b) 48, (c) 72 h.

In this assay, a wound is created on a monolayer of cultured mammalian cells, and cell migration is monitored [46].

In our study, the control group did not receive the amphiphilic block copolymer. As shown in the figure, the wound created in the control group closed after 72 h. In the cell lines treated with the amphiphilic block copolymer, the wound also closed after 72 h, similar to the control group. The anti-metastatic activity of the block copolymer, compared with the control group, is shown in Figs. 4–7 and does not demonstrate a significant difference. The invasion assay results

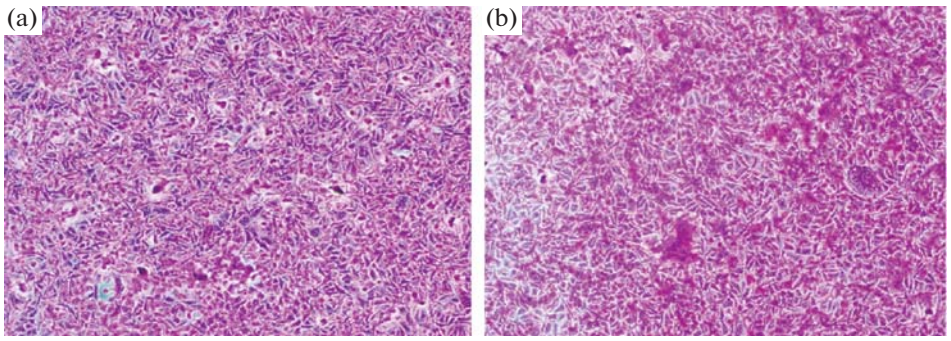

Fig. 6. Control group (non copolymer treated) MDA-MB-231 cell line: (a) 48, (b) 72 h.

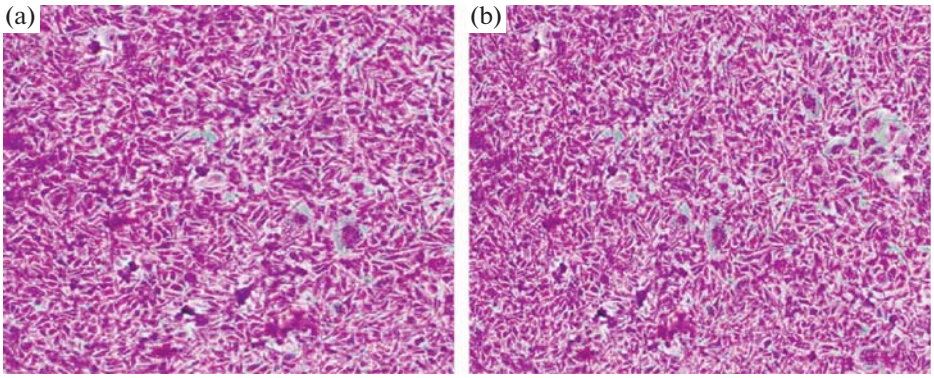

Fig. 7. Copolymer treated MDA-MB-231 cell line: (a) 48, (b) 72 h.

indicated that the molecule did not inhibit the invasion of triple-negative breast cancer cells.

CONCLUSIONS

In this study, a novel bifunctional initiator, 1,2-bis[(3-oxapropyl)oxa]benzene, which has not been previously reported in polymerization reactions, was successfully employed for the synthesis of an ABA-type block copolymer (PNIPAM-*b*-PLLA-*b*-PNIPAM) via a combination of ring-opening polymerization (ROP) and atom transfer radical polymerization (ATRP). The initiator's aromatic core introduces chromophoric properties that are absent in conventional aliphatic initiators, enabling spectroscopic monitoring and offering a foundation for the development of photo-responsive functionalities. Furthermore, its electron-rich aromatic ring is amenable to post-polymerization modifications such as azo-coupling or electrophilic substitution, thereby facilitating targeted conjugation with bioactive molecules. The rigid and symmetrical structure of the initiator contributes to precise control over block copolymer architecture, resulting in lower polydispersity indices and enhanced micellar stability—characteristics highly desirable for biomedical applications. Structural characterization of the synthesized polymers was conducted using FTIR and ^{1}H NMR spectroscopy, and the number-average molecular weight (M_n) determined from NMR peak integrals was consistent with theoretical values. Notably, the resulting PNIPAM-*b*-PLLA-*b*-PNIPAM exhibited non-toxic behavior, underlining its potential as a drug delivery platform in anticancer applications.

FUNDING

This study was supported by Kırşehir Ahi Evran University Scientific Research Projects Unit. Project number: MMF.A2.24.001.

CONFLICT OF INTEREST

The authors of this work declare that they have no conflicts of interest.

REFERENCES

1. M. Chehelgerdi and A. Doosti, J. Nanobiotechnol. **18**, 63 (2020).
2. S. Bayda, M. Adeel, T. Tuccinardi, M. Cordani, and F. Rizzolio, Molecules **25**, 112 (2019).

3. S. S. Das, P. Bharadwaj, M. Bilal, M. Barani, A. Rahdar, P. Taboada, S. Bungau, and G. Z. Kyzas, Polymers **12**, 1397 (2020).
4. F. Shams, A. Golchin, A. Azari, A. L. Mohammadi, F. Zarein, A. Khosravi, and A. Ardeshirylajimi, Mol. Biol. Rep. **49**, 1389 (2022).
5. T. M. Allen and P. R. Cullis, Science **303**, 1818 (2004).
6. N. Bertrand, J. Wu, X. Xu, N. Kamaly, and O. C. Farokhzad, Adv. Drug Delivery Rev. **66**, 2 (2014).
7. A. N. Lukyanov and V. P. Torchilin, Adv. Drug Delivery Rev. **56**, 1273 (2004).
8. H. Cabral, K. Miyata, K. Osada, and K. Kataoka, Chem. Rev. **118**, 6844 (2018).
9. D. Dutta, W. Ke, L. Xi, W. Yin, M. Zhou, and Z. Ge, Nanomed. Nanobiotechnol. **12**, e1585 (2020).
10. B. Kumar, K. Jalodia, P. Kumar, and H. K. Gautam, J. Drug Delivery Sci. Technol. **41**, 260 (2017).
11. S. S. Agasti, S. Rana, M. H. Park, C. K. Kim, C. C. You, and V. M. Rotello, Adv. Drug Delivery Rev. **62**, 316 (2010).
12. P. Yang, S. Zhang, N. Zhang, Y. Wang, J. Zhong, X. Sun, Y. Qi, X. Chen, Z. Li, and Y. Li, ACS Appl. Mater. Interfaces **11**, 42671 (2019).
13. K. Letchford and H. Burt, Eur. J. Pharm. Biopharm. **65**, 259 (2007).
14. S. Rawal and M. M. Patel, J. Control. Release **301**, 76 (2019).
15. L. Zhao, N. Li, K. Wang, C. Shi, L. Zhang, and Y. Luan, Biomaterials **35**, 1284 (2014).
16. F. Su, P. Yun, C. Li, R. Li, L. Xi, Y. Wang, Y. Chen, and S. Li, Colloids Surf*., A* **566**, 120 (2019).
17. N. N. Zashikhina, M. V. Volokitina, V. A. Korzhikov-Vlakh, I. I. Tarasenko, A. Lavrentieva, T. Scheper, E. Rühl, R. V. Orlova, T. B. Tennikova, and E. G. Korzhikova-Vlakh, Eur. J. Pharm. Sci. **109**, 1 (2017).
18. K. Kamenova, E. Haladjova, G. Grancharov, M. Kyulavska, V. Tzankova, D. Aluani, K. Yoncheva, S. Pispas, and P. Petrov, Eur. Polym. J. **104**, 1 (2018).
19. X. B. Xiong, Z. Binkhathlan, O. Molavi, and A. Lavasanifar, Acta Biomater. **8**, 2017 (2012).
20. V. Mikhalevich, I. Craciun, M. Kyropoulou, C. G. Palivan, and W. Meier, Biomacromolecules **18**, 3471 (2017).
21. M. Levit, N. Zashikhina, A. Vdovchenko, A. Dobrodumov, N. Zakharova, A. Kashina, E. Rühl, A. Lavrentieva, T. Scheper, T. Tennikova, and E. Korzhikova-Vlakh, Polymers **12**, 183 (2020).
22. K. Jankova, M. Bednarek, and S. Hvilsted, J. Polym. Sci. Part A: Polym. Chem. **43**, 3748 (2005).
23. S. Wan, J. Huang, H. Yan, and K. Liu, J. Mater. Chem. **16**, 298 (2006).
24. W. Tang and K. Matyjaszewski, Macromolecules **40**, 1858 (2007).
25. Y. Y. Tong, Y. Q. Dong, F. S. Du, and Z. C. Li, Macromolecules **41**, 7339 (2008).
26. J. Hegewald, J. Pionteck, L. Häußler, H. Komber, and B. Voit, J. Polym. Sci. Part A: Polym. Chem. **47**, 3845 (2009).
27. W. Van Camp, H. Gao, F. E. Du Prez, and K. Matyjaszewski, J. Polym. Sci. Part A: Polym. Chem. **48**, 2016 (2010).
28. M. Lammens, D. Fournier, M. W. Fijten, R. Hoogenboom, and F. D. Prez, Macromol. Rapid Commun. **30**, 2049 (2009).
29. E. Aliyev, S. Shishatskiy, C. Abetz, Y. J. Lee, S. Neumann, T. Emmler, and V. Filiz, Adv. Mater. Interfaces **7**, 2000443 (2020).
30. M. Mısır, Y. S. Savaskan, and A. Bilgin, Polymers **15**, 3813 (2023).
31. D. L. Patton and R. C. Advincula, Macromolecules **39**, 8674 (2006).
32. A. C. Albertsson and I. K. Varma, Biomacromolecules **4**, 1466 (2003).
33. I. Navarro-Baena, A. Marcos-Fernández, A. Fernández-Torres, J. M Kenny, and L. Peponi, RSC Adv. **4**, 8510 (2014).
34. Y. Hu, V. Darcos, S. Monge, and S. Li, J. Polym. Sci. Part A: Polym. Chem. **51**, 3274 (2013).
35. N. Karanikolopoulos, M. Zamurovic, M. Pitsikalis, and N. Hadjichristidis, Biomacromolecules **11**, 430 (2010).
36. R. S. Lee, C. H. Lin, I. A. Aljuffali, K. Y. Hu, and J. Y. Fang, J. Nanobiotechnol. **13**, 42 (2015).
37. E. Ayano, M. Karaki, T. Ishihara, H. Kanazawa, and T. Okano, Colloids Surf*., B* **99**, 67 (2012).
38. D. Zhang, Y. Xia, H. Gong, D. Zhang, X. Chen, S. Shi, and L. Lei, J. Nanosci. Nanotechnol. **21**, 2174 (2021).
39. Q. Fu, T. G. McKenzie, S. Tan, E. Nam, and G. G. Qiao, Polym. Chem. **6**, 5362 (2015).
40. D. D. Perrin and W. L. F. Armarego, *Purification of Laboratory Chemicals*, 2nd ed. (Pergamon Press Oxford, UK, 1989).
41. A. Bilgin, D. Yanmaz, and C. Yagci, Turk. J. Chem. **38**, 1135 (2014).
42. L. M. Shaw, in *Cell Migration: Developmental Methods and Protocols*, Ed. by C. M. Wells and M. Parsons (Springer Science, 2005), p. 97.
43. H. Vargas-Villagran, A. Romo-Uribe, E. Teran-Salgado, M. Dominguez-Diaz, and A. Flores, Polym. Bull. **71**, 2437 (2014).
44. H. L. Gong, L. Lei, S.-X. Shi, Y.-Z. Xia, and X.-N. Chen, J. Nanosci. Nanotechnol. **18**, 3266 (2018).
45. A. Ali, R. Bhadane, A. A. Asl, C.-E. Wilén, O. Salo-Ahen, J. M. Rosenholm, and K. K. Bansal, RSC Adv. **12**, 26763 (2022).
46. Y. K. Suh, A. Robinson, N. Zanghi, A. Kratz, A. Gustetic, M. M. Crow, T. Ritts, W. Hankey, and V. A. Segarra, J. Microbiol. Biol. Educ. **23**, e00061-22 (2022).